

## Scaling Shift in Multicracked Fiber Bundles

Fabio Manca,<sup>1</sup> Stefano Giordano,<sup>1,2</sup> Pier Luca Palla,<sup>1,3</sup> and Fabrizio Cleri<sup>1,3</sup>

<sup>1</sup>*Institute of Electronics, Microelectronics and Nanotechnology (IEMN, UMR 8520), 59652 Villeneuve d'Ascq, France*

<sup>2</sup>*International Associated Laboratory LIA LEMAC/LICS, ECLille, 59652 Villeneuve d'Ascq, France*

<sup>3</sup>*University of Lille I, 59652 Villeneuve d'Ascq, France*

(Received 12 May 2014; published 16 December 2014)

Bundles of fibers, wires, or filaments are ubiquitous structures in both natural and artificial materials. We investigate the bundle degradation induced by an external damaging action through a theoretical model describing an assembly of parallel fibers, progressively damaged by a random population of cracks. Fibers in our model interact by means of a lateral linear coupling, thus retaining structural integrity even after substantial damage. Monte Carlo simulations of the Young's modulus degradation for increasing crack density demonstrate a remarkable scaling shift between an exponential and a power-law regime. Analytical solutions of the model confirm this behavior, and provide a thorough understanding of the underlying physics.

DOI: 10.1103/PhysRevLett.113.255501

PACS numbers: 62.20.M-, 46.50.+a, 46.65.+g, 89.75.Da

Fiber bundle assemblies are structural elements largely present in both natural materials and technological applications. Nature has extensively exploited the mechanical properties of filamentary biopolymers, such as cytoskeletal proteins, F-actin, or microtubules, for many crucial processes in eukaryotic cells [1]. At the tissue length scale we find bundle structures like collagen, spider silk, bone, tendon, muscle, all exhibiting uncommon qualities, including the rare combination of large strength and high toughness [2–4]. These materials take advantage of specific features, such as the hierarchical assemblage [5], the twisted structure [6], and the degree of disorder that may increase the overall strength [7]. Artificial materials aiming at high mechanical performances have often taken inspiration from biomaterials, such as carbon nanotube that have been used as building blocks for novel assembled systems [8,9].

Given their interest as structural materials, mechanical failure in bundles is a major subject of study [10,11]. The “fiber-bundle model” (FBM), originally developed to study the failure of spun cotton yarns [12], was extended to consider parallel fibers with statistically distributed strength [13]. There, when an external load produces the failure of a fiber, its fraction of load is equally redistributed among all the intact fibers (global load sharing). A complementary statistical and time-dependent phenomenological theory has been proposed in Refs. [14,15]. Another redistribution strategy is the so-called local load sharing, stating that the load of a broken fiber is carried only by the nearest intact fibers [16]. Exactly solvable models based on this rule have been largely investigated [17–19]. It is well known that global and local rules lead to completely different statistical behaviors [20–24]. The FBM approach has been smartly modified in order to account for the matrix viscoelasticity with a power-law creep compliance [25,26], the plasticity [27,28], the nonlinear creeping matrix [29], the

brittle-to-ductile transition [30], and the complexity of specific heterogeneous structures [31,32].

In this context, the mechanical degradation induced by external agents, such as chemicals or radiations, is crucial to understand the resistance of bundle materials to variable environmental constraints. As prominent examples, spanning widely different fields, one could cite the degradation induced by some antibiotics in tendon collagen [33], or the lysis of muscle sarcomeres produced by some statins [34], damage in the form of single- and double-strand breaks in DNA irradiated by high-energy photons in cancer radiotherapy [35,36], or degraded by a restriction enzyme [37]. At more macroscopic scales, examples include corrosion of high-voltage power cable bundles [38], or suspended-bridge steel cables [39], corrosion of steel bundles and meshes in concrete structures [40], loss of cohesion in tree-root bundles with variable soil wetness, triggering shallow landslides [41,42].

In this Letter, we investigate a fiber-bundle assembly of arbitrary geometry, with  $M$  parallel fibers characterized by the linear longitudinal response and lateral coupling; the fibers undergo localized damages, in the form of  $N$  random breaks affecting the overall Young's modulus. Notably, broken fibers in our model do not lose entirely their cohesion with the bundle, thanks to the lateral coupling  $k$ , an essential ingredient to model realistic structures. Although the progressive damage originated by the load redistribution is a relevant effect largely studied within the FBM [10,11], we have not included this feature in order to isolate the statistical behavior induced by the random fractures within the interacting fibers. Under this respect, the problem belongs to the field of homogenization theories [43–47]. In particular, our approach allows us to demonstrate the existence of a marked shift in the scaling law of the effective Young's modulus of the fiber bundle: the

elastic modulus decays with an exponential scaling,  $\exp(-N/M)$  at small  $N$ , and goes into a power-law scaling  $1/N^2$  at increasing values of  $N$ . The threshold  $N^*$  between the exponential and the power-law regime is a decreasing function of the lateral coupling  $k$ . This “slowing-down” shift has therefore important practical implications, in that the yielding of a fiber-bundle material could be postponed to longer times upon increasing the amount of lateral coupling in the bundle.

Let us consider a bundle of  $M$  intact parallel fibers of length  $l$ , arbitrarily arranged on their cross section, for instance a flat [Fig. 1(a)], or a circular bundle [Fig. 1(b)]. The system can be described by the balance equations

$$\frac{\partial T_i(x)}{\partial x} = -G_i(x), \quad \frac{\partial U_i(x)}{\partial x} = \frac{1}{E_i} T_i(x), \quad (1)$$

for  $i = 1, \dots, M$  and  $0 \leq x \leq l$ , where

$$G_i(x) = \sum_{j=1}^M k_{ij} (U_j - U_i). \quad (2)$$

Here,  $T_i(x)$  is the scalar stress,  $U_i(x)$  the longitudinal displacement,  $E_i$  the Young modulus of the  $i$ th fiber, and  $k_{ij}$  are the lateral coupling coefficients [Fig. 1(c)]. The structure of the matrix  $k_{ij}$  introduces the most general coupling rule, being able to define the local, the global, and all intermediate interaction schemes. Defining  $\vec{\zeta}$  as the vector containing all the variables  $(T_1, U_1, T_2, U_2, \dots, T_M, U_M)$ , the system of equations can

be written in the more compact form  $d\vec{\zeta}/dx = \mathbf{A}\vec{\zeta}$ , where  $\mathbf{A}$  is a  $2M \times 2M$  constant matrix. Therefore, the behavior of an intact bundle segment can be studied by means of the matrix exponential  $\exp(\mathbf{A}x)$ .

Let us now introduce a population of  $N$  breaks at the arbitrary positions  $x_i$ ,  $i = 1, \dots, N$ . We assume that the fracture located at  $x_i$  is assigned to the  $j_i$ th fiber of the bundle ( $j_i \in \{1, 2, \dots, M\}$ ,  $\forall i = 1, \dots, N$ ). We also define for convenience  $x_0 = 0$  (left end of the bundle) and  $x_{N+1} = l$  (right end of the bundle). It is important to remark that when a fiber is broken in one or more points it continues to contribute to the overall stiffness of the bundle through the lateral interactions with the other fibers. Under such assumptions, we can identify  $N + 1$  intact segments of the entire bundle, for any  $x \in (x_i, x_{i+1})$ ,  $\forall i = 0, \dots, N$ . Hence, for each of the above intervals we can write  $\vec{\zeta}(x_{i+1}^-) = \exp[\mathbf{A}(x_{i+1} - x_i)]\vec{\zeta}(x_i^+)$ . The fiber breaks are described by the following boundary conditions for  $x = x_i$  ( $i = 1, \dots, N$ ):  $U_k(x_i^-) = U_k(x_i^+) \forall k \neq j_i$  and  $T_k(x_i^-) = T_k(x_i^+) \forall k \neq j_i$ , representing, respectively, the continuity of displacement, and stress, in the intact fibers. Moreover,  $T_{j_i}(x_i^-) = 0$  and  $T_{j_i}(x_i^+) = 0$ , meaning that there is no transmission of force across the broken fiber. We maintain fixed the left end of the bundle [ $U_k(x_0) = 0$ ] and we prescribe a given displacement to its right end [ $U_k(x_{N+1}) = \delta$  where  $\delta$  is a parameter]. If we rearrange the quantities  $\vec{\zeta}(x_0)$ ,  $\vec{\zeta}(x_1^-)$ ,  $\vec{\zeta}(x_1^+)$ ,  $\vec{\zeta}(x_2^-)$ ,  $\dots$ ,  $\vec{\zeta}(x_{N-1}^-)$ ,  $\vec{\zeta}(x_N^-)$ ,  $\vec{\zeta}(x_N^+)$ ,  $\vec{\zeta}(x_{N+1})$  in a vector  $\vec{\eta}$  we obtain a system  $\mathbf{B}\vec{\eta} = \vec{b}$  with  $4M(N + 1)$  unknowns (it can be shown that  $\mathbf{B}$  is always nonsingular). For a given distribution of fiber breaks, the effective Young modulus of the overall bundle can be obtained as  $E_{\text{eff}} = (1/\delta) \sum_{k=1}^M T_k(l)$ , which represents the effective modulus of a single fiber equivalent to the whole degraded bundle.

The most general problem dealing with  $M$  fibers and  $N$  randomly distributed breaks can only be solved numerically through Monte Carlo (MC) simulations. We generate a large number of break distributions for each given  $M$ ,  $N$  and bundle geometry, from which we calculate the average Young modulus  $\langle E_{\text{eff}} \rangle$  of the bundle. In the MC simulations we took  $E_i = E$  for all fibers and  $k_{ij} = k$  for each couple of neighboring fibers (local coupling). The relative strength of the longitudinal versus lateral interaction was set by the value of the reduced variable  $\xi^2 = kl^2/E$ , ranging from 0.045 to 8, to span almost three decades. For both the flat and the circular bundle we set  $7 \leq M \leq 19$  (see Fig. 1).

The degradation behavior of  $\langle E_{\text{eff}} \rangle$  as a function of  $N$  can be summarized by the MC results displayed in Fig. 2 in which two specific degradation regimes can be clearly identified: for low values of  $N$ , the straight lines in the semilog plot of Fig. 2 correspond to an exponential scaling; for larger values of  $N$ , the straight lines in the log-log plot (inset) correspond to a power-law scaling (Fig. 2 shows

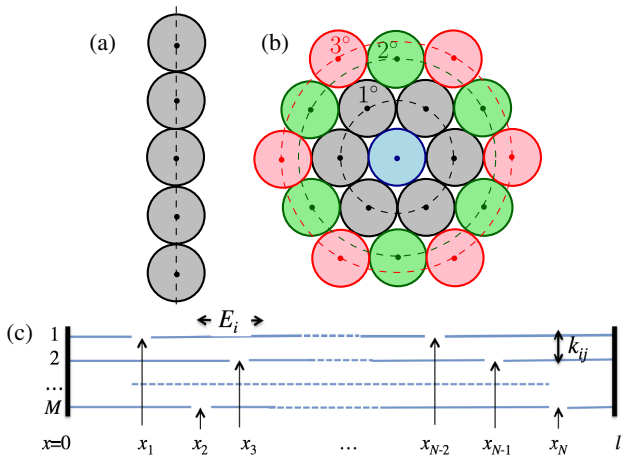


FIG. 1 (color online). Cross-sectional view of the bundle structures. In both the flat (a) and in the circular bundle (b), we considered  $M$  fibers with  $7 \leq M \leq 19$  (note that  $M = 7, 13, 19$  in the circular bundle correspond to exactly one, two, or three shells of neighbors). In (c) the arrangement of  $M$  parallel fibers of length  $l$  with  $N$  breaks at  $x_1, \dots, x_N$  is shown;  $E_i$  is the longitudinal (Young) elastic modulus of the  $i$ th fiber, and  $k_{ij}$  is the lateral coupling modulus of the pair  $ij$ .

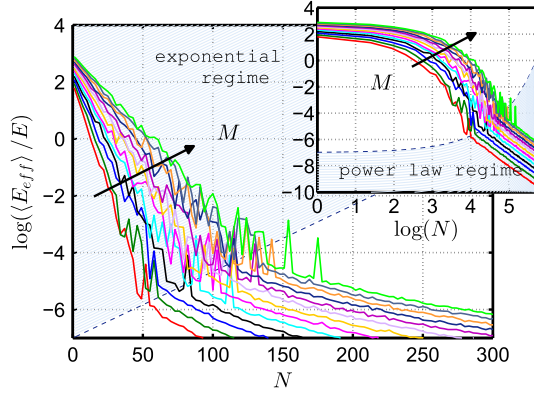


FIG. 2 (color online). Monte Carlo results for  $\langle E_{\text{eff}} \rangle / E$  versus  $N$  in semilogarithmic (main plot) and bilogarithmic (inset) scales. We considered  $kl^2/E = 0.045$  and 13 values of  $M$ , from 7 to 19.

results only for the flat bundle and  $\xi^2 = 0.045$ , the results for other cases being entirely similar).

The shift between these two scaling regimes is, indeed, a very interesting feature, since it marks the passage from a very fast (exponential) decrease of  $\langle E_{\text{eff}} \rangle(N)$  to a much slower degradation, in what may be called a slowing-down shift for the loss of structural integrity. In Fig. 3 we report the results of MC simulations for the flat bundle with  $M = 19$ , for a discrete range of values of  $\xi^2 = 0.045$  to 8. It can be seen that the shift at  $N^*$  is very sharp for the smallest values of  $k$ , and becomes smoother for higher values of the lateral coupling constant (increasing  $\xi^2$ ). However,  $N^*$  decreases logarithmically upon increasing  $\xi^2$ , showing that an increase in the amount of lateral interaction between the fibers (even fragmented) anticipates the slowing-down shift to earlier stages of the degradation. We remark that we observed this shift behavior also with nonlocal couplings among the fibers. It is interesting to note that similar regimes were observed in multicracked bulk solid materials [45–47], for which it was separately found that randomly oriented cracks lead to an exponential degradation, while

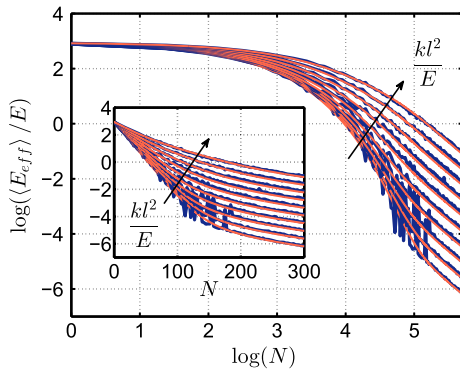


FIG. 3 (color online). Monte Carlo results (noisy blue lines) and theoretical interpolation (continuous red lines) for  $\langle E_{\text{eff}} \rangle / (ME)$  versus  $N$  for different values of  $kl^2/E$  (0.045, 0.08, 0.14, 0.25, 0.45, 0.8, 1.4, 2.5, 4.5, and 8) and  $M = 19$  (flat bundle).

parallel cracks lead to a power-law decay of the effective properties.

The physics behind these two limiting regimes can be elucidated by looking at two extreme conditions for which a fully analytical solution to the model can be provided. First, we consider just two interacting fibers, in which  $N/2$  breaks are regularly and alternately distributed in each fiber of length  $l$ . In this simple, idealized case the model can be explicitly solved, obtaining

$$\frac{E_{\text{eff}}(N)}{2E} = \frac{1}{1 + 2f_N(\sqrt{2}\xi)}, \quad (3)$$

where

$$f_N(z) = \frac{1}{z} \tanh\left(\frac{z}{N+1}\right) + \frac{N-1}{z} \coth\left(\frac{z}{N+1}\right) + \frac{N-1}{z} \operatorname{csch}\left(\frac{z}{N+1}\right). \quad (4)$$

We observe that, for  $N$  approaching infinity,  $E_{\text{eff}}(N)$  goes to zero with the power law  $E_{\text{eff}} \sim kl^2/N^2$ . Moreover, it is important to recognize that, at large  $N$ , the decrease of  $E_{\text{eff}}$  does not depend on the Young modulus  $E$  of the fibers, but is dominated by the lateral interactions among the adjacent fragments of the broken fibers. This underscores the major role of the lateral interaction  $k$  in determining the scaling shift at  $N^*$ .

As a second, analytically solvable case, we consider the system composed of  $M$  noninteracting fibers ( $k = 0$ ), with  $N$  randomly distributed breaks among all the fibers with probability  $1/M$ . Since lateral interactions are now absent, when a fiber is broken at one or more sites its contribution to the effective stiffness  $\langle E_{\text{eff}} \rangle$  is zero. We calculate the probability to have  $n_1$  breaks on the first fiber,  $n_2$  breaks on the second one, and so forth. Since there are  $N!/(n_1! \cdot \dots \cdot n_M!)$  sequences of  $N$  breaks yielding the particular distribution  $\{n_1, \dots, n_M\}$  (with  $\sum_{i=1}^M n_i = N$ ), we find such a probability to be  $\Pr\{n_1, \dots, n_M\} = N!/(n_1! \cdot \dots \cdot n_M! M^N)$ . We can therefore determine the probability  $\mathcal{P}_s(N)$  to have  $s$  intact fibers after producing  $N$  random breaks in the bundle. If this is the case, in each distribution  $\{n_1, \dots, n_M\}$  there are  $s$  zeros and  $M - s$  strictly positive numbers. Since there are  $\binom{M}{s}$  combinations of such  $s$  zeros within the distribution  $\{n_1, \dots, n_M\}$ , we eventually obtain

$$\mathcal{P}_s(N) = \binom{M}{s} \sum_{\sum_{i=1}^{M-s} n_i = N} \frac{N!}{n_1! \cdot \dots \cdot n_{M-s}!} \frac{1}{M^N}. \quad (5)$$

This expression for the probability can be summed, to obtain the following result in closed form:

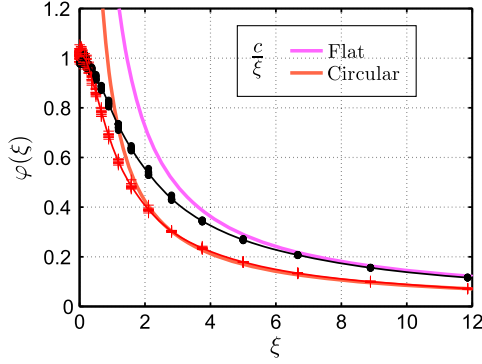


FIG. 4 (color online). Numerical determination of the function  $\varphi(\xi)$  defined in Eq. (8). The black curve (flat bundle) and the red curve (circular bundle) are asymptotically converging to  $\varphi(\xi) = c/\xi$  with  $c = 1.45$  (flat bundle) and  $c = 0.85$  (circular bundle).

$$\mathcal{P}_s(N) = \frac{M!}{s!M^N} \mathcal{S}_N^{M-s}, \quad (6)$$

where  $\mathcal{S}_n^m$  is the Stirling number of the second kind. This last equation can be used to prove that the probabilities  $\mathcal{P}_s(N)$  generate a complete probability space, i.e.,  $\sum_{s=0}^M \mathcal{P}_s(N) = 1$ . From the same equation, we obtain an explicit expression for the effective Young's modulus of the fiber bundle in the absence of lateral interactions

$$\frac{\langle E_{\text{eff}} \rangle}{ME} = \frac{1}{M} \sum_{s=0}^M s \mathcal{P}_s(N) = \left( \frac{M-1}{M} \right)^N \cong e^{-N/M}, \quad (7)$$

the last approximation being valid for large values of  $M$ . This second analytical result shows that the mechanical degradation in a bundle of noninteracting fibers follows an exponential law in the single variable  $N/M$ .

The above two limiting results allow us to formulate appropriate scaling functions with free parameters, by which the whole results of MC simulations for any bundle geometry, size  $M$ , and interaction strength  $\xi^2$ , can be represented. In fact, the exponential regime at small values of  $N$  is described by

$$\log \frac{\langle E_{\text{eff}}^{\text{exp}} \rangle}{ME} = -\varphi(\xi) \frac{N}{M^{\alpha}}, \quad (8)$$

with  $\varphi(\xi)$  a function, to be determined by fitting the MC results, which describes the early-stage degradation of the bundle stiffness  $\langle E_{\text{eff}} \rangle$  as a function of the relative interaction strength  $\xi = \sqrt{k l^2 / E}$ . The shape of the function  $\varphi(\xi)$  extracted from the MC simulations is shown in Fig. 4, for the flat and circular bundle geometries. The value  $\varphi(0) = 1$  is coherent with Eq. (7), when  $k = 0$ . The function is universal for a large enough  $M$  (in practice, already for  $M \gtrsim 10$ ), and goes into the asymptotic behavior  $\varphi(\xi) \sim c/\xi$  at large  $\xi$ , the value of  $c$  depending on the

TABLE I. Parameters and scaling exponents characterizing the fast (exponential) and slow (power-law) degradation regimes.

	Parallel bundle	Circular bundle
$\alpha$	$0.97 \pm 0.06$	$1.05 \pm 0.12$
$a$	$0.40 \pm 0.06$	$0.40 \pm 0.07$
$b$	$2.09 \pm 0.11$	$2.08 \pm 0.21$
$\beta$	$2.29 \pm 0.19$	$2.61 \pm 0.35$
$\nu$	$1.97 \pm 0.25$	$1.91 \pm 0.37$

geometry ( $c = 1.45$  for the flat, and  $c = 0.85$  for the circular bundle, respectively).

On the other hand, the power-law regime at larger  $N$  can be described by

$$\frac{\langle E_{\text{eff}}^{\text{pow}} \rangle}{ME} = a \frac{M^{\beta} \left( \sqrt{\frac{k l^2}{E}} \right)^{\nu}}{N^b}. \quad (9)$$

The best fit of the free parameters  $\alpha$ ,  $a$ ,  $b$ ,  $\beta$  and  $\nu$  in Eqs. (8)–(9) from the numerical MC simulations are reported in Table I. Coherently with Eq. (7),  $\alpha = 1$ , thus extending to any value of  $k$  the analytical result for  $k = 0$ , at small  $N$ . In the same way, the fitted value  $b = 2$  confirms for any value of  $M$  the  $1/N^2$  scaling, analytically obtained for  $M = 2$ . Furthermore, the value  $\nu = 2$  obtained by the best fit allows us to explain the loss of significance of  $E$ , and the parallel increase of importance of  $k$  in determining the asymptotic effective stiffness  $\langle E_{\text{eff}} \rangle$ : indeed, for  $\nu = 2$  the  $E$  appearing in the rhs and lhs of Eq. (9) cancel out each other. Therefore, the physical explanation of the shift towards a slower (power-law) degradation regime would be that increasingly small fiber fragments are only weakly deformed, and the effective Young modulus is eventually determined by their interactions.

Finally, Eqs. (8) and (9) can be unified in a single function  $\langle E_{\text{eff}} \rangle / ME = \mathcal{E} + 1/(r/N + 1/\mathcal{P})$ , where  $\mathcal{E} = \langle E_{\text{eff}}^{\text{exp}} \rangle / ME$  from Eq. (8), and  $\mathcal{P} = \langle E_{\text{eff}}^{\text{pow}} \rangle / ME$  from Eq. (9). The switching between the two regimes is controlled by the coefficient  $r$ , which assumes the values  $1.0 \times 10^3$  for the flat bundle and  $3.0 \times 10^3$  for the circular one. This function is the origin of the continuous lines in Fig. 3, nicely representing the MC simulations over the entire range of parameters.

In the present Letter, we discussed a purely elastic system. Nevertheless, we have also studied a time-invariant viscoelastic coupling, described by a complex valued  $k$  under a permanent sinusoidal regime. Again, we observed the scaling shift between the exponential and power-law responses at  $N^*$ , which is now a decreasing function of the viscosity (further details will be published elsewhere). Other refined models for the viscoelastic behavior should be adopted to analyze more realistic structures, e.g., the power-law creep compliance [25,26], the plasticity [27,28], and the nonlinear creeping [29].

In conclusion, we predicted the existence of an unprecedented exponential to power-law slowing-down shift in the degradation of a multicroaked bundle. The lateral interaction among the fibers is the key ingredient in triggering this shift as a function of the crack density  $N$ . Notably, the critical value  $N^*$  can be lowered by increasing the interaction strength, a relevant feature for practical purposes. For example, in radiation [36] or chemical [37] damage of DNA bundles for cancer radiotherapy, the knowledge of the degradation dynamics is useful to properly design therapy protocols. In related experiments, an exponential degradation has been measured, which exactly corresponds to the first regime found in our investigation [36,37]. Moreover, a strong dependence on the viscosity of the solution has been observed concerning the degradation velocity of the mechanical response. Although no quantitative results are presently available, there are indications that larger values of the viscosity in strongly degraded DNA bundles lead to a complex nonexponential dynamics, which could correspond to a scaling shift induced by denser buffer media. Similarly, at entirely different time and length scales, it has been observed that soil strength decreases exponentially with increasing soil wetness [42] (i.e., reducing the effective interaction), showing signs of breakdown under very dry soil conditions.

- 
- [1] S. M. Rafelsky and J. A. Theriot, *Annu. Rev. Biochem.* **73**, 209 (2004).
- [2] B. L. Smith, T. E. Schaffer, M. Viani, J. B. Thompson, N. A. Frederick, J. Kindt, A. Belcher, G. D. Stucky, D. E. Morse, and P. K. Hansma, *Nature (London)* **399**, 761 (1999).
- [3] P. Fratzl, *Curr. Opin. Colloid Interface Sci.* **8**, 32 (2003).
- [4] Y. Liu, Z. Shao, and F. Vollrath, *Nat. Mater.* **4**, 901 (2005).
- [5] M. Buehler, *Nano Today* **5**, 379 (2010).
- [6] G. M. Grason, *Phys. Rev. Lett.* **105**, 045502 (2010).
- [7] S. W. Cranford, *J. R. Soc. Interface* **10**, 0148 (2013).
- [8] L. Liu, W. Ma, and Z. Zhang, *Small* **7**, 1504 (2011).
- [9] S. Kumar *et al.*, *Macromolecules* **35**, 9039 (2002).
- [10] S. Pradhan, A. Hansen, and B. K. Chakrabarti, *Rev. Mod. Phys.* **82**, 499 (2010).
- [11] H. Kawamura, T. Hatano, N. Kato, S. Biswas, and B. K. Chakrabarti, *Rev. Mod. Phys.* **84**, 839 (2012).
- [12] F. T. Peirce, *J. Text. Ind.* **17**, T355 (1926).
- [13] H. E. Daniels, *Proc. R. Soc. London, Ser. A* **183**, 405 (1945).
- [14] B. D. Coleman, *J. Appl. Phys.* **27**, 862 (1956).
- [15] B. D. Coleman, *J. Appl. Phys.* **29**, 968 (1958).
- [16] D. G. Harlow and S. L. Phoenix, *J. Compos. Mater.* **12**, 195 (1978).
- [17] D. G. Harlow and S. L. Phoenix, *J. Mech. Phys. Solids* **39**, 173 (1991).
- [18] D. Sornette, *J. Phys. A* **22**, L243 (1989).
- [19] P. M. Duxbury and P. L. Leath, *Phys. Rev. B* **49**, 12676 (1994).
- [20] S. Zapperi, P. Ray, H. E. Stanley, and A. Vespignani, *Phys. Rev. Lett.* **78**, 1408 (1997).
- [21] M. Kloster, A. Hansen, and P. C. Hemmer, *Phys. Rev. E* **56**, 2615 (1997).
- [22] P. Bhattacharyya, S. Pradhan, and B. K. Chakrabarti, *Phys. Rev. E* **67**, 046122 (2003).
- [23] J. B. Gómez, D. Iñiguez, and A. F. Pacheco, *Phys. Rev. Lett.* **71**, 380 (1993).
- [24] D. H. Kim, B. J. Kim, and H. Jeong, *Phys. Rev. Lett.* **94**, 025501 (2005).
- [25] D. C. Lagoudas, C. Y. Hui, and S. L. Phoenix, *Int. J. Solids Struct.* **25**, 45 (1989).
- [26] I. J. Beyerlein, S. L. Phoenix, and R. Raj, *Int. J. Solids Struct.* **35**, 3177 (1998).
- [27] F. Raischel, F. Kun, and H. J. Herrmann, *Phys. Rev. E* **73**, 066101 (2006).
- [28] I. J. Beyerlein and S. L. Phoenix, *J. Mech. Phys. Solids* **44**, 1997 (1996).
- [29] D. D. Mason, C. Y. Hui, and S. L. Phoenix, *Int. J. Solids Struct.* **29**, 2829 (1992).
- [30] K. Kovács, R. C. Hidalgo, I. Pagonabarraga, and F. Kun, *Phys. Rev. E* **87**, 042816 (2013).
- [31] K. S. Gjerden, A. Stormo, and A. Hansen, *Phys. Rev. Lett.* **111**, 135502 (2013).
- [32] Z. Danku and F. Kun, *Phys. Rev. Lett.* **111**, 084302 (2013).
- [33] Y. Kashida and M. Kato, *Antimicrob. Agents Chemother.* **41**, 2389 (1997).
- [34] P. Cao, J.-i. Hanai, P. Tanksale, S. Imamura, V. P. Sukhatme, and S. H. Lecker, *FASEB J.* **23**, 2844 (2009).
- [35] J. F. Ward, *Int. J. Radiat. Biol.* **57**, 1141 (1990).
- [36] G. Perret *et al.*, in *Engineering in Medicine and Biology Society (EMBC), 35th Annual International Conference, Osaka, 2013*, (IEEE, New York, 2013), p. 6820.
- [37] M. Kumemura *et al.*, in *International Conference on Micro Electro Mechanical Systems (MEMS), Cancún* (IEEE, New York, 2011).
- [38] E. S. Ibrahim, *Electric Power Systems Research* **52**, 9 (1999).
- [39] R. Betti, A. West, G. Vermaas, and Y. Cao, *J. Bridge Eng.* **10**, 151 (2005).
- [40] J. P. Broomfield, *Corrosion of Steel in Concrete* (Taylor & Francis, New York, 2007).
- [41] D. Cohen, P. Lehmann, and D. Or, *Water Resour. Res.* **45**, W10436 (2009).
- [42] Y. Matsushi and Y. Matsukura, *Bull. Eng. Geol. Env.* **65**, 449 (2006).
- [43] S. Torquato, *Random Heterogeneous Materials* (Springer-Verlag, New York, 2002).
- [44] M. Kachanov and I. Sevostianov, *Int. J. Solids Struct.* **42**, 309 (2005).
- [45] S. Giordano and L. Colombo, *Phys. Rev. Lett.* **98**, 055503 (2007).
- [46] R. Spatschek, C. Gugenberger, and E. A. Brener, *Phys. Rev. B* **80**, 144106 (2009).
- [47] S. Giordano and P. L. Palla, *Eur. Phys. J. B* **85**, 59 (2012).